Investigating Land Surface Temperature Variation and Land Use Land Cover Changes in Pathumthani, Thailand (1997-2023) using Landsat Satellite Imagery: A Comprehensive Analysis of LST and Urban Hot Spots (UHS)

Thammaboribal, P.
Asian Institute of Technology, P.O. Box 4, 58 Moo 9, Km. 42, Paholyothin Highway, Klong Luang, Pathum Thani 12120 Thailand
E-mail: *prapasgnss@gmail.com*

DOI: https://doi.org/10.52939/ijg.v20i2.3063

Abstract

This study explores the dynamic transformations in land use and land cover (LULC), land surface temperature (LST), and the spatial distribution of Urban Hot Spots (UHSs) in Pathumthani from 1997 to 2023. Landsat satellite imagery was utilized for the analysis, employing the Maximum Likelihood classifier for LULC classification. The research reveals a substantial surge in built-up areas, particularly notable with a twofold increase in 2023 compared to 1997, concentrated along the north-south axis. While vegetation remains the dominant land cover, it experienced an initial increase from 2004 to 2023, followed by a declining trend. Nevertheless, vegetation constitutes over 60% of the total area, concentrated in the eastern and western regions. In summary, the spatial distribution of UHS in 1997 exhibited dispersion across the study area. However, starting from 2004, there was a noticeable concentration of UHSs within built-up areas, particularly in the northern part, coinciding with the presence of the Navanakorn industrial zone. Urban development encroachment into Muang Pathumthani, Thanyaburi, and Lam Luk Ka districts led to the emergence of UHSs in the southern part, mirroring the trajectory of urban sprawl. This southern section, adjacent to Bangkok and in proximity to Don Muang airport, witnessed UHS emergence due to urban expansion, notably influenced by the development of the mass rapid transit (MRT) connecting Pathumtani and Bangkok. The study highlights the importance of studying Land Surface Temperature (LST) to identify areas with higher temperatures, contributing valuable insights for urban planning and strategies to mitigate heat-related challenges in the region.

Keywords: Landsat, Land use land cover, LST, LULC, Pathumthani, UHS

1. Introduction

The investigation of Land Surface Temperature (LST) and Land Use/Land Cover (LULC) changes holds paramount significance in contemporary environmental research, playing a pivotal role in understanding the complex interplay between natural processes and human activities. These analyses are essential for unraveling the intricate dynamics that govern our planet's surface and are crucial components in addressing pressing issues related to climate change, urbanization, and sustainable land management LST serves as a key indicator of the thermal behavior of the Earth's surface [1][2][3][4][5][6][7] and [8]. Fluctuations in LST are influenced by a myriad of factors, including solar radiation, land cover types, elevation [9], and human activities. Monitoring LST provides critical insights into the impacts of climate change and human-induced alterations on local and regional microclimates [10]. As the Earth's climate undergoes unprecedented changes, studying LST becomes indispensable for predicting and adapting to the evolving thermal conditions, mitigating the effects of urban heat islands, and informing sustainable land use practices [11] and [12].

Simultaneously, LULC changes serve as a barometer for assessing the transformations in the Earth's surface brought about by human activities. Urbanization, agricultural expansion, and deforestation are examples of LULC changes that have profound implications for ecosystems, biodiversity, and climate patterns. Investigating these changes is crucial for understanding the drivers behind alterations in land cover, predicting future trends, and formulating informed policies for sustainable resource management and conservation [13].

The integration of LST and LULC change analyses is particularly powerful, offering a comprehensive view of how human-induced and natural factors converge to shape the Earth's surface conditions [14] and [15]. The thermal implications of land cover alterations, such as the impact of urbanization on local temperatures or the role of vegetation in moderating surface heat, can be unveiled through this combined approach [16]. In a world grappling with the impacts of climate change and rapid urbanization, conducting LST and LULC change studies becomes not just an academic pursuit but a practical necessity. These investigations provide valuable data for climate scientists, urban planners, policymakers, and environmentalists alike. Ultimately, understanding the dynamics of LST and LULC changes is instrumental in formulating strategies for sustainable development, fostering resilient communities, and preserving the delicate balance between human activities and the natural environment [17] and [18].

Pathumthani, a central province in Thailand, has undergone significant transformations in both land surface temperature (LST) and land use/land cover (LULC) over the past decade. This study leverages the Landsat satellite series to examine the temporal dynamics of LST from 2010 to 2023 and its interplay with LULC changes, providing a comprehensive analysis of how environmental factors influence thermal patterns in the region. Landsat's high spatial and temporal resolution offers an unparalleled opportunity to monitor and understand the evolving landscape. The period under investigation coincides with a noteworthy chapter in Pathumthani's history, marked by urban expansion, agricultural intensification, and shifting land-use patterns. LULC changes, encompassing transitions between natural, agricultural, and urban areas, have profound implications for local microclimates and subsequently impact LST. This study seeks to unravel the intricacies of these changes, offering insights into the complex relationship between human activities and environmental dynamics.

As urban areas expand and agriculture practices evolve, the thermal characteristics of the land surface respond accordingly. The analysis of LST in conjunction with LULC changes allows us to discern the thermal implications of alterations in land cover types. Additionally, understanding how vegetation and built-up structures influence LST is vital for assessing the overall health and sustainability of the environment [19]. In this research, we embark on a journey to identify trends, hotspots, and potential driving forces behind the observed LST variations in Pathumthani. The amalgamation of advanced remote sensing techniques, Landsat's temporal coverage, and comprehensive LULC change analyses equips us to offer valuable insights into the region's environmental dynamics. The findings are expected to contribute significantly to the ongoing discourse on sustainable land management, climate resilience, and urban planning in Pathumthani and beyond.

2. Study Area

Pathum Thani, a province in the central region of Thailand as illustrates in Figure 1, serves as a compelling study area for research on LULC change and LST. This region, located just north of Bangkok, holds economic and cultural significance, contributing to the overall vitality of the nation. Its geographic composition includes a mix of urban and rural landscapes, featuring areas of industrial development, residential zones, and agricultural expanses [20].

As an economically vibrant province, Pathum Thani is poised for dynamic LULC changes driven by factors such as population growth, industrialization, and evolving agricultural practices. Understanding these land use patterns is crucial for unraveling the economic dynamics and urbanization trends within the region. Additionally, its proximity to Bangkok suggests that the province may experience the Urban Heat Island (UHI) effect, where urban areas exhibit higher temperatures than surrounding rural areas. Investigating LST can provide valuable insights into the extent of this phenomenon and its environmental implications. Pathum Thani boasts diverse environmental features, including water bodies, green spaces, and natural habitats. The study of LULC changes becomes instrumental in assessing the impact of human activities on these ecosystems. Furthermore, the tropical climate of Pathum Thani, characterized by distinct wet and dry seasons, adds a layer of complexity to the relationship between land use changes and climate variability.

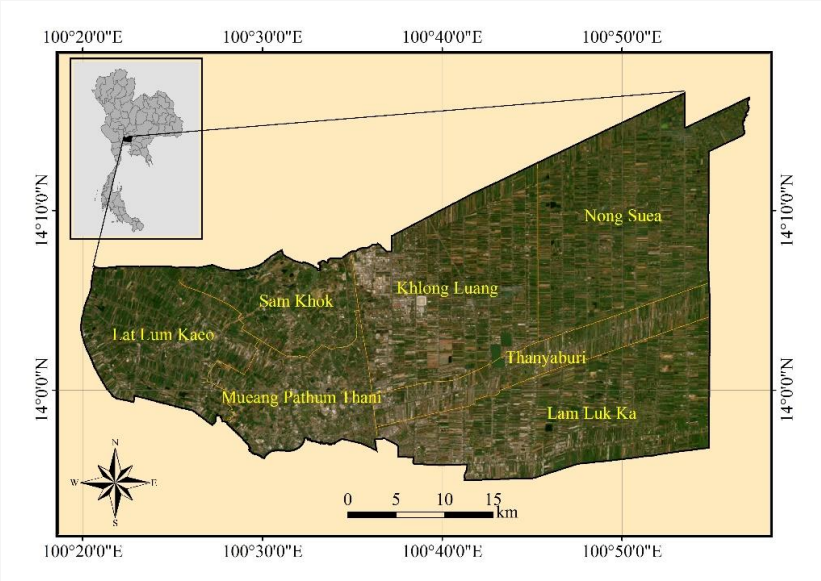

Figure 1: Study area in Pathumthani, Thailand

Table 1: Landsat satellites band designations [21]

Landsat 4-5 TM Landsat 7 ETM+		Landsat 8-9 OLI/TIRS	
		Band 1	Coastal/Aerosal
Band 1	Blue	Band 2	Blue
Band 2	Green	Band 3	Green
Band 3	Red	Band 4	Red
Band 4	NIR	Band 5	NIR
Band 5	SWIR-1	Band 6	SWIR-1
Band 6	TIR	Band 10	TIR-1
		Band 11	TIR-2
Band 7	SWIR-2	Band 7	SWIR-2
Band 8	Pan	Band 8	Pan
		Band 9	Cirrus

3. Methodology

3.1 Data Collection

This research is dedicated to examining the time series of LST in Pathumthani province of Thailand by analyzing land cover changes and vegetation loss. The selected periods for analysis are 1997 2003, 2012, 2018, and 2023, and the objective is to understand the evolution of surface temperature over this timeframe. Landsat 5, 7, and 8 image data were acquired for the specified years, and the LULC was classified into four categories: (1) built-up areas; (2) vegetation areas; (3) water body; and (4) bare land.

The classification of Land Use/Land Cover (LULC) employed a supervised classification technique known as "maximum likelihood." Both visible bands (R-G-B) and near-infrared (NIR) bands were incorporated in the LULC classification process. Furthermore, a thermal band was employed to estimate LST values. The satellite imagery was obtained from USGS EarthExplorer, accessible at https://earthexplorer.usgs.gov/. The details of the Landsat series employed in this study are outlined in Table 1. According to Table 1, the description of each Landsat series as well as and their respective band spatial resolutions are as follows:

Landsat 4-5 Thematic Mapper (TM) images comprise seven spectral bands with a spatial resolution of 30 meters for Bands 1 to 5 and 7. Band 6, the thermal infrared band, has a spatial resolution of 120 meters but is resampled to 30-meter pixels.

Landsat 7 Enhanced Thematic Mapper Plus (ETM+) images consist of eight spectral bands with a 30-meter spatial resolution for Bands 1 to 7. Band 8 (panchromatic) has a higher resolution of 15 meters. All bands offer two gain settings (high or low) for increased radiometric sensitivity and dynamic range, except for Band 6, which collects both high and low gain for all scenes.

Landsat 8 Operational Land Imager (OLI) and Thermal Infrared Sensor (TIRS) images include nine spectral bands with a 30-meter spatial resolution for Bands 1 to 7 and 9. The new Band 1 (ultra-blue) is valuable for coastal and aerosol studies, and Band 9 aids in cirrus cloud detection. Band 8 (panchromatic) maintains a higher resolution of 15 meters. Thermal bands 10 and 11, crucial for precise surface temperature measurements, have a native resolution of 100 meters, but they are resampled to 30 meters to align with the spatial resolution of other bands. Landsat 9 instruments are enhanced duplicates of those on Landsat 8 [22].

The Earth's surface experiences dynamic changes throughout the year, including variations in solar angle, vegetation cover, and atmospheric conditions. The followings are the factors that might affect the LST analysis.

- Seasonal Changes: Different seasons bring about variations in surface characteristics such as vegetation growth, land cover, and water availability. These changes can significantly impact LST, and comparing data collected at different times of the year may introduce confounding factors that hinder accurate analysis.

- Solar Angle: The angle and intensity of sunlight vary with the seasons, affecting how surfaces absorb and emit thermal radiation. Consistent timing of satellite imagery acquisition helps maintain a similar solar angle, ensuring more reliable comparisons of LST over time.

- Vegetation Dynamics: Vegetation plays a crucial role in regulating surface temperature through processes like evapotranspiration. Seasonal changes in vegetation cover influence the thermal properties of the land surface. Collecting imagery in the same period helps control for these variations.

- Atmospheric Conditions: Atmospheric conditions, such as humidity and cloud cover, can impact the accuracy of thermal measurements. Acquiring data during the same period helps minimize the impact of these atmospheric variables, leading to more consistent and comparable results.

- Long-Term Trends: Monitoring LST over an extended period with consistent timing enables the identification of long-term trends and patterns, providing valuable insights into climate-related changes, urban heat island effects, and other environmental phenomena.

Therefore, the satellite imagery was gathered between 1997 and 2023, specifically during the summer season, encompassing the hottest months of the year, from March to May to maintain a consistent time frame for satellite imagery collection in LST analysis which allows for more accurate and meaningful comparisons. The data acquisition dates are presented in Table 2. The images were obtained with minimal cloud cover, accounting for less than 10%.

3.2 Land Use Land Cover Classification

Land use and land cover (LULC) classification through satellite imagery involves the categorization of different Earth surface types based on their spectral characteristics, as captured by remote sensing satellites. The process plays a crucial role in monitoring and understanding landscape changes over time. Initially, satellite imagery is acquired and preprocessed to correct for atmospheric effects and geometric distortions. Subsequently, representative areas known as Regions of Interest (ROIs) are selected, and spectral information is extracted to create a training dataset for the classification algorithm [22].

The maximum likelihood algorithm, a widely utilized technique for LULC classification [23], is employed in the next steps. This algorithm calculates the probability of a pixel belonging to a specific land cover class by assuming that the spectral values for each class follow a normal distribution. The pixel is then assigned to the class with the highest probability, facilitating the creation of a classified image. Feature selection is essential to choose the most relevant spectral bands for input to the algorithm, maximizing the separability of different land cover classes.

Table 2: Data acquisition dates

No.	Year	Acquisition dates	Landsat series
1	1997	24 April 1997	Landsat 5 TM
2	2004	26 March 2004	Landsat 5 TM
3	2012	11 May 2012	Landsat 7 ETM+
4	2018	18 April 2018	Landsat 8 OLI/TIRS
5	2023	18 May 2023	Landsat 8 OLI/TIRS

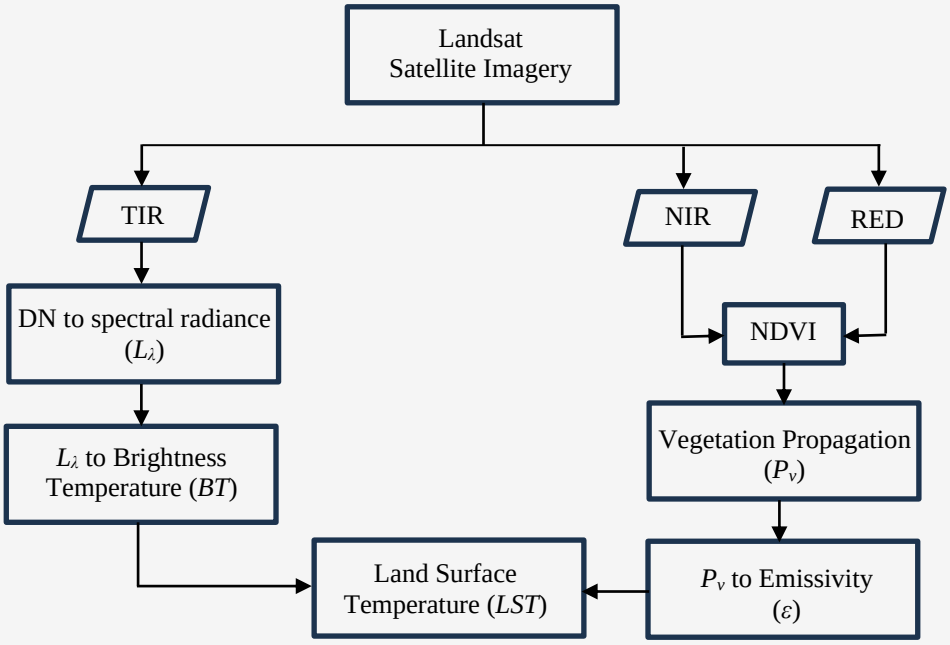

Figure 2: Determination of land surface temperature (LST) using Landsat satellite imagery

The effectiveness of the maximum likelihood algorithm relies on adhering to the assumptions of normality and equal covariance matrices for spectral signatures and requires a supervised approach with training samples for each land cover class [24][25] and [26]. In this study, the LULC were categorized into 4 classes namely built-up area, vegetation area, waterbody, and bareland.

3.3 Data Processing

The objective of this study is to investigate LST variation and LULC change as well as the relation between LST and NDVI in Pathumthani from 1997 to 2023 using Landsat satellite imagery. The schematic depicting the process of determining LST from Landsat satellite imagery is illustrated in Figure 2. As per the schematic presented in Figure 2, the steps for determining Land Surface Temperature (LST) are outlined as follows:

The satellite imagery was downloaded from EarthExplorer, a platform provided by the United States Geological Survey (USGS) accessible at https://earthexplorer.usgs.gov/. The acquisition dates of the data are presented in Table 2. Convert the digital number (DN) of the thermal infrared band (TIR) to spectral radiance (L_λ) using Equation 1:

$$L_\lambda = \left(\frac{LMAX_\lambda - LMIN_\lambda}{QcalMAX - QcalMIN} \right) (Qcal - QcalMIN) + LMIN_\lambda$$

Equation 1

where:

L_λ is top of atmospheric radiance in $Wm^{-2}sr^{-1}\mu m^{-1}$

$LMAX_\lambda$ is spectral radiance scales to $QcalMAX$ [17.04]

$LMIN_\lambda$ is spectral radiance scales to $QcalMIN$ [0]

$QcalMAX$ is maximum quantized calibrated pixel value [255]

$QcalMIN$ is minimum quantized calibrated pixel value [0 for the products processed before 4/5/2004 and 1 for the products processed after 4/5/2004]

$Qcal$ is digital number of the thermal band [DN]

Equation 1 is applied for the digital number (DN) conversion of Landsat 4-5TM and Landsat 7ETM+. Alternatively, if Landsat 8OLI imagery is employed, the top-of-atmosphere radiance is determined using Equation 2:

$$L_\lambda = M_L Q_{cal} + A_L$$

Equation 2

Where:

M_L is band specific multiplicative rescaling factor (RADIANCE_MULT_BAND_x) obtained from the metadata

A_L is band specific additive calling factor (RADIANCE_ADD_BAND_x) obtained from the metadata

Qcal is digital number [*DN*]

When utilizing Band 10 of Landsat 8 in the study, the M_L and A_L values are 0.0003342 and 0.1, respectively. Therefore, Equation 2 can be simplified to Equation 3:

$$L_\lambda = 0.0003342 Q_{cal} + 0.1$$

Equation 3

The top of atmospheric radiance (TOA) derived from equation 1 to equation 3 is converted into brightness temperature using Equation 4.

$$BT = \frac{K_2}{\ln\left[\frac{K_1}{L_\lambda} + 1\right]} - 273.15$$

Equation 4

Where:

BT is brightness temperature [°C]

K_1 is band specific thermal conversion constant (K1_CONSTANT_BAND_x)

K_2 is band specific thermal conversion constant (K2_CONSTANT_BAND_x)

The constants K_1 and K_2 of each Landsat series presents in Table 3. The quantity of vegetation is crucial in estimating Land Surface Temperature (LST) [28]. To assess this, the Normalized Difference Vegetation Index (NDVI) becomes imperative. NDVI serves as an indicator of vegetation health by evaluating how plant cell structures reflect light waves in both the near-infrared band (NIR) and red band (RED). Equation 5 is used to calculate NDVI.

$$NDVI = \frac{NIR - RED}{NIR + RED}$$

Equation 5

Proportion of vegetation (P_V) refers to the proportion or fraction of an area that is covered by vegetation. It is a measure that quantifies the extent of plant cover within a specific area. This concept is commonly used to assess and monitor vegetation cover in landscapes, ecosystems, or regions [29]. P_V is determined from Equation 6.

$$P_V = \left(\frac{NDVI - NDVI_{\min}}{NDVI_{\max} - NDVI_{\min}}\right)^2$$

Equation 6

Where $NDVI_{max}$ and $NDVI_{min}$ are the maximum and minimum of NDVI, respectively.

Land surface emissivity (ε) is a key factor in LST analysis. It refers to the efficiency with which a surface emits thermal radiation. In the context of remote sensing and thermal infrared imagery, every object with a temperature above absolute zero emits electromagnetic radiation. The rate at which this radiation is emitted depends on the emissivity of the surface. For LST analysis, emissivity is crucial because it influences the accuracy of temperature measurements derived from thermal infrared data. Different surfaces have different emissivity values, and emissivity is typically between 0 and 1 [30]. A surface with an emissivity of 1 is a perfect emitter (blackbody), while a surface with an emissivity of 0 is a perfect reflector.

Accurate knowledge of surface emissivity is particularly important when analyzing temperature variations in different types of landscapes and land cover. There are several models that utilize to determine the land surface emissivity from NDVI.

Table 3: Band specific thermal conversion constants [27]

Constant	Landsat 5	Landsat 7	Landsat 8 (B10)
K_1 ($Wm^{-2}sr^{-1}\mu m^{-1}$)	607.76	666.09	774.89
K_2 (Kelvin)	1,260.56	1,282.71	1,321.08

Sobrino et al., [31] formulated an improved equation for calculating land surface emissivity. The equation utilizes the mean value for soil emissivity from the ASTER spectral library (http://asterweb.jpl.nasa.gov), as presented in Equation 7.

$$\varepsilon = 0.004P_V + 0.986$$

Equation 7

Mono window algorithm as presented in Equation 8 allows the determination of Land Surface Temperature (LST).

$$LST = \frac{BT}{1+\left[\lambda \frac{BT}{\rho}\right] Ln(\varepsilon)}$$

Equation 8

Where:

BT is brightness temperature determined from Equation 4

λ is wavelength of the TIR band

ρ is constant [14,380]

Urban hot spot (UHS) is a localized area within an urban environment where temperatures are particularly high or where the effects of the urban hot spots are more pronounced. These hot spots may occur due to specific factors such as intense human activities, specific land use patterns, or variations in surface materials [32]. UHS is defined in equation 10 [33].

$$LST > \mu + 2\sigma$$

Equation 9

Where μ and σ are the mean and standard deviation of LST, respectively. The area where the LST surpasses the threshold specified in equation 10 is designated as an UHS.

4. Results and Discussion

4.1 LULC changes from 1997 to 2023

In this study, the LULC were categorized into four classes: water body, built-up area, vegetation area, and bare land. The LULC classification employed the maximum likelihood classifier, the LULC classification employed the maximum likelihood classifier, and the corresponding results are presented in Figure 3, and the details of land use land cover (LULC) changes are presented in Table 4 and Figure 4. Figure 3 unmistakably illustrates a noteworthy surge in built-up areas spanning the temporal interval from 1997 to 2023. The augmentation of the built-up area in 2023 exhibits a twofold increase when juxtaposed with the corresponding 1997 values, notably along the north-south axis, particularly evident along Paholyothin Rd in the Klongluang district and Ransit-Nakornnayok Rd in the Thanyaburi district. Figures 3, 4, and Table 4 illustrate that the predominant land cover in the study area is characterized as vegetation. In 2004, the vegetation area increased from 960.35 km² to 1196.03 km², but subsequently exhibited a declining trend from 2004 to 2023. Nevertheless, vegetation still comprises more than 60% of the total area. The vegetation areas are predominantly located in the eastern and western regions of Pathumthani, specifically in Nong Suea and Lad Lum Kaew districts, respectively.

A notable transformation in bareland was observed between 1997 and 2004. In 1997, bareland accounted for 22.25% of the area, but by 2004, it had reduced significantly to 2.29%, maintaining a range of 2%-6% thereafter. The built-up area exhibited a gradual increase from 1997 to 2018, with the built-up area covering 25% of the province in 2023. Conversely, the water body area did not undergo significant changes from 1997 to 2023, consistently occupying approximately 1%-3% of the total area. The variability in bareland area alterations was indeterminate; as depicted in Figure 3, bareland regions exhibited a stochastic distribution within the vegetation area on an annual basis. The seemingly random occurrence of bareland can likely be attributed to agricultural activities such as cultivation and plowing of crops within the vegetation area, leading to the observation of small-scale bareland pockets within these vegetated regions.

4.2 LST Variation from 1997 to 2023

Figure 5 depicts high temperature in LST for the years 1997, 2004, and 2023, surpassing that observed in 2012 and 2018. The findings further indicate that the LST in 2023 is the highest recorded since 1997, reaching 45 °C. Particularly, heightened LST regions were discerned within the built-up area, notably along the north-south axis encompassing Paholyothin Rd. and along Rangsit-Nakornnayok Rd. in the eastern segment of the study area. Additionally, each annual high LST region was consistently observed within the built-up area, contrasting with the comparatively lower temperatures noted in the vegetation area. The LST statistics extracted from Figure 5 are presented in Table 5 and Figure 6. Table 5 and Figure 6 describe the LST across the years 1997, 2004, 2012, 2018, and 2023. A discernible trend is evident, wherein the average LST exhibits a gradual decrease from 1997 to 2018, reaching its lowest at 31.3 °C in 2018, and upswing to the highest of 38.5 °C in 2023.

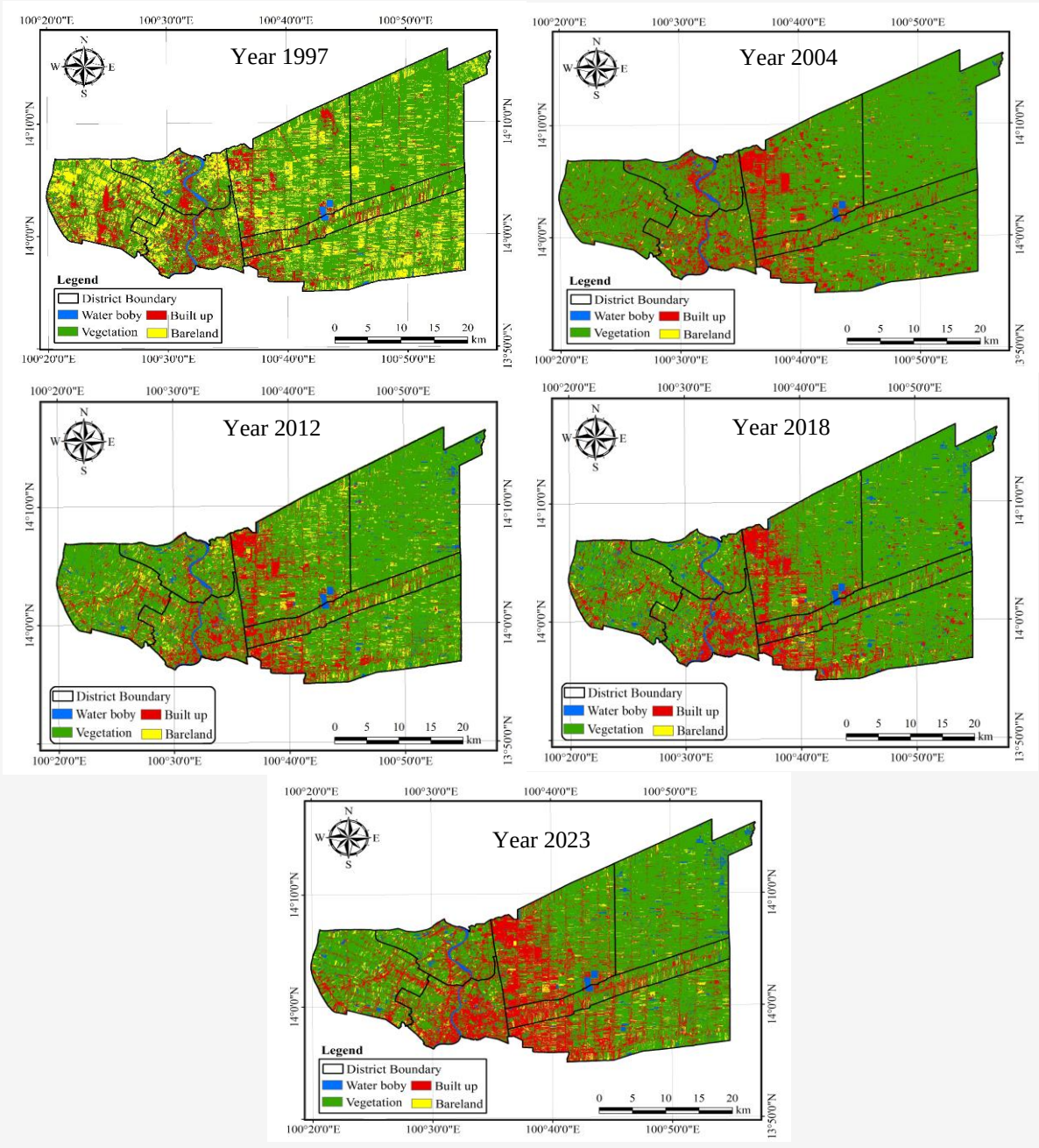

Figure 3: LULC of Pathumthani change from 1997 to 2023

Table 4: Areas of LULC in Pathumthani from 1997 to 2023

Year	Built up		Vegetation		Bareland		Water body	
	km²	%	km²	%	km²	%	km²	%
1997	190.94	12.58	960.35	63.29	345.20	22.75	20.90	1.38
2004	265.02	17.47	1196.03	78.82	34.77	2.29	21.58	1.42
2012	272.29	17.94	1146.19	75.54	60.99	4.02	37.92	2.50
2018	279.81	18.44	1125.67	74.18	59.77	3.94	52.14	3.44
2023	384.74	25.36	995.37	65.60	96.99	6.39	40.30	2.66

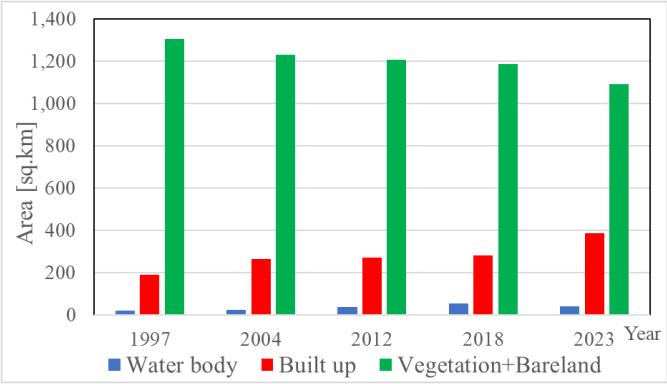

Figure 4: LULC Area changes in Pathumthani from 1997 to 2023

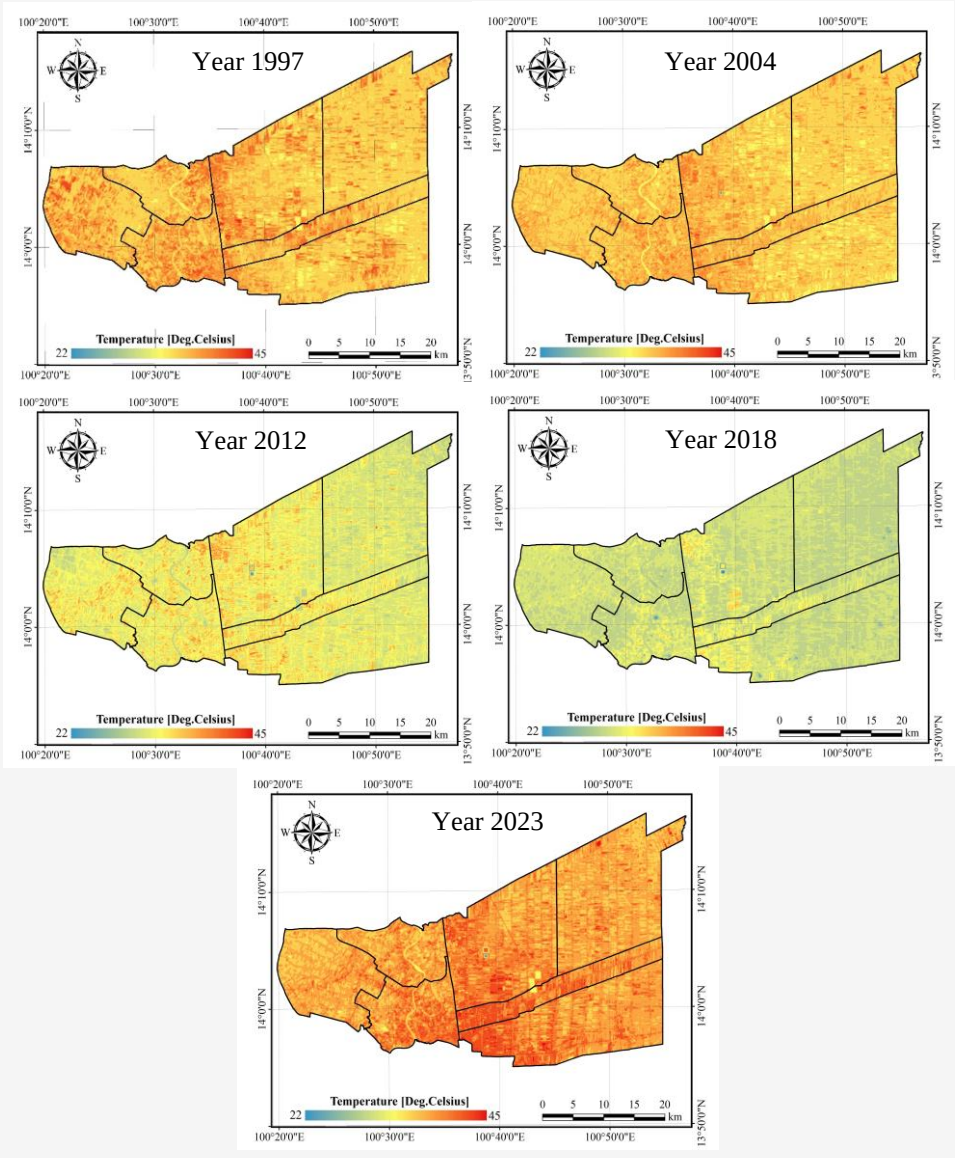

Figure 5: LST variation of Pathumthani from 1997 to 2023

Table 5: LST statistics of Pathumthani, Thailand from 1997 to 2023

Year	Min [°C]	Max [°C]	Mean [°C]	SD [°C]
1997	31.8	43.4	37.4	1.8
2004	23.0	42.8	36.7	1.4
2012	22.7	40.7	33.6	1.9
2018	20.7	38.8	31.3	1.2
2023	22.8	45.2	38.5	1.8

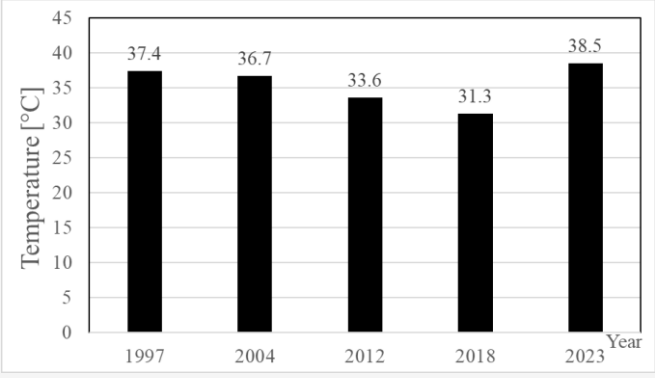

Figure 6: Average LST of Pathumthani

The average LST difference in 2018 (the lowest) and 2023 (the highest) was 7.2 °C. Notably, these findings appear incongruous with the prevailing global climate scenario, characterized by an overarching trend of escalating temperatures attributed to the phenomenon of global warming.

El Niño and La Niña represent climate patterns in the eastern tropical Pacific. These phenomena are delineated by the Oceanic Niño Index (ONI), recognized as the standard by the National Oceanic and Atmospheric Administration (NOAA). Calculated from the running 3-month average sea surface temperature (SST) anomaly within the Niño3.4 region, spanning 5°N to 5°S and 120°W to 170°W, the ONI serves as a key metric for assessing these climatic events. The phenomena are characterized by five consecutive overlapping 3-month periods with temperatures either at or above a +0.5°C anomaly for warm (El Niño) events or at or below a -0.5°C anomaly for cool (La Niña) events. The threshold is classified into different categories: Weak (0.5 to 0.9 SST anomaly), Moderate (1.0 to 1.4), Strong (1.5 to 1.9), and Very Strong (≥ 2.0) events [34].

According to ONI provided by NOAA, available at https://ggweather.com/enso/oni.htm, it is evident that El Niño phenomena did not occur in 1997 and 2004. Consequently, LST difference between these two years amounted to 0.7°C. La Niña events were observed in 2012 and 2018, contributing to lower LST values compared to 1997 and 2004.

In 2023, there was a substantial increase in LST compared to 2018, indicating elevated temperatures across the study area. The heightened LST in 2018 resulted from a moderate El Niño event. Although Thailand is not directly impacted by El Niño and La Niña phenomena, during El Niño periods, the country may experience elevated temperatures beyond normal levels, potentially leading to adverse weather events in specific areas [35] and [36]. It can be summarized that the typical average LST for Pathumthani is expected to fall within the range of 36-37.5 °C.

4.3 UHS from 1997 to 2023

In this investigation, UHSs were employed to delineate areas characterized by elevated LST within the designated study region. A UHS is defined as a location where the LST surpasses two standard deviations above the average LST. As illustrated in Figure 5, the UHSs were dispersed across the study area in 1997. However, starting from 2004 and continuing through subsequent years, the UHSs became concentrated within built-up areas. Specifically, in 2004 and 2012, UHSs were observed predominantly in the northern part, coinciding with the location of the Navanakorn industrial zone, covering 1,040 hectares on Km.46 of Paholyothin highway in Khlong Luang district. The encroachment of urban development into Muang Pathumthani, Thanyaburi, and Lam Luk Ka districts led to the southern part of the study area experiencing UHSs, mirroring the direction of urban sprawl.

This southern section, adjacent to Bangkok—the capital of Thailand—and in proximity to Don Muang airport, witnessed UHS emergence due to urban expansion. Notably, the development of the mass rapid transit (MRT) connecting Pathumtani and Bangkok contributed significantly to urban sprawl in the southern direction. In 2023, numerous housing estates have emerged in the southern part of the study area, specifically in the Lam Luk Ka district. Additionally, expansive housing estate developments were observed in Khlong Sam (Canal no.3), a sub-district of Thanyaburi district situated in the central region of the study area. Figure 7 illustrates that UHSs were predominantly observed in the housing estate areas and occasionally in the industrial zone.

Figure 7: UHSs of Pathumthani from 1997 to 2023

This is because the surface of housing estate is considerable rougher than that of industrial zone. Rough surfaces generally absorb more heat than smooth surfaces. Rough surfaces have a larger surface area and, consequently, more areas for incident radiation to be absorbed [37]. The increased surface area allows for greater absorption and retention of heat. In contrast, smooth surfaces reflect more sunlight and absorb less heat due to their reduced surface area and higher reflectivity. The specific material properties, color, and composition of the surfaces also play a role in their heat absorption characteristics [38]. Dark-colored surfaces tend to absorb more heat than light-colored ones, as they absorb a greater portion of the incident solar radiation [39]. Consequently, UHSs) exhibit a tendency to manifest in housing estates rather than other LULC types.

5. Conclusion

The study reveals a substantial increase in built-up areas from 1997 to 2023, with a particularly noteworthy twofold surge observed in 2023 compared to 1997. This urban expansion is most pronounced along the north-south axis, prominently visible along Paholyothin Rd in the Klongluang district and Ransit-Nakornnayok Rd in the Thanyaburi district. While the dominant land cover in the study area is characterized as vegetation, the vegetation area experienced an initial increase from 2004 to 2023, although showing a declining trend thereafter. Nevertheless, vegetation continues to constitute over 60% of the total area, with concentrations in the eastern and western regions of Pathumthani, specifically in Nong Suea and Lad Lum Kaew districts.

LST data can provide insights into local climate trends and changes. Monitoring temperature variations over time is essential for understanding the impact of climate change on the region. Higher land surface temperatures can have health implications, particularly during heatwaves. Investigating LST can help identify areas prone to extreme temperatures, allowing for better public health planning and response strategies. LST data is also valuable for monitoring environmental changes, including land cover modifications and vegetation health. This information is vital for sustainable land management practices and biodiversity conservation. Additionally, LST data is essential for urban planners to design resilient and sustainable cities. It helps identify heat-prone areas and supports the implementation of green infrastructure and other measures to enhance urban livability.

The spatial distribution of UHSs in 1997 showed dispersion throughout the study area. However, from 2004 onward, there was a notable concentration of UHSs within built-up areas. Specifically, in 2004 and 2012, UHSs were predominantly observed in the northern part, aligning with the location of the Navanakorn industrial zone. Urban development encroachment into Muang Pathumthani, Thanyaburi, and Lam Luk Ka districts resulted in UHSs emerging in the southern part, mirroring the direction of urban sprawl. The southern section, adjacent to Bangkok and in proximity to Don Muang airport, witnessed UHS emergence due to urban expansion, notably influenced by the development of the mass rapid transit (MRT) connecting Pathumtani and Bangkok. The spatial evolution of UHSs in the study area reflects the dynamic interplay between urban development, surface characteristics, and heat absorption. The findings underscore the significance of considering land use and surface properties in understanding the distribution of urban hot spots and their potential implications for local climates. Pathumthani may experience the UHS, where urban areas tend to be warmer than their rural surroundings. Studying LST can help identify areas with higher temperatures, contributing to urban planning and mitigating heat-related issues.

References

[1] Khalil, U., Aslam, B., Azam, U. and Khalid, H. M. D., (2012). Time Series Analysis of Land Surface Temperature and Drivers of Urban Heat Island Effect Based on Remotely Sensed Data to Develop a Prediction Model. *Applied Artificial Intelligence*. Vol. 35(15), 1803-1828. https://doi.org/10.1080/08839514.2021.1993633.

[2] Moisa, M. B., Gabissa, B. T., Hinkosa, L. B., Dejene, I. N. and Gemeda, D. O., (2022). Analysis of Land Surface Temperature Using Geospatial Technologies in Gida Kiremu, Limu, and Amuru District, Western Ethiopia. *Artificial Intelligence in Agriculture*. Vol. 6, 90-99. https://doi.org/10.1016/j.aiia.2022.06.002.

[3] Wongwan, W. and Pongsawat, S., (2023). Analysis of Correlation between the Land Surface Temperature, the Land-use and Land-Cover in Mueang District, Lampang Province. *Journal of Advanced Development in Engineering and Science*. Vol. 13(36), 38-53. https://ph03.tci-thaijo.org/index.php/pitjournal/article/view/578.

[4] Mansourmoghaddam, M., Rousta, I., Zamani, M. and Olafsson, H., (2023). Investigating and Predicting Land Surface Temperature (LST) Based on Remotely Sensed Data During 1987–2030 (A case study of Reykjavik city, Iceland). *Urban Ecosyst*., Vol. 26(2), 337-359. https://doi.org/10.1007/s11252-023-01337-9.

[5] Ordoñez, C. A. and Silva, D., (2023). Land Use/Land Cover (LULC), change Detection, and Simulation Analysis of Manila Bay's Dolomite Mining Site in Cebu, Philippines Using Sentinel–2 Satellite. *International Journal of Geoinformatics*. Vol. 19(5), 87-103. https://doi.org/10.52939/ijg.v19i5.2667.

[6] Arunplod, C., Phonphan, W., Wongsongja, N., Utarasakul, T., Niemmanee, T., Daraneesrisuk, J. and Thongdara, R., (2023). Spatial Dynamics Evolution of Land Use for the Study of the Local Traditional Living Changes. *International Journal of Geoinformatics*, Vol. 19(4), 37-49. https://doi.org/10.52939/ijg.v19i4.2635.

[7] Sharaf El Din, E., Elsherif, A., Ramadan, S. and Aboelkhair, H., (2023). Mapping of Thermal Indices Using an Automated Landsat 8-based-ArcGIS Model: A Case Study in Alexandria City, Egypt. *International Journal of Geoinformatics*, Vol. 19(9), 1–12. https://doi.org/10.52939/ijg.v19i9.2823.

[8] Jaelani, L. and Handayani, C., (2022). Spatio-temporal Analysis of Land Surface Temperature Changes in Java Island from Aqua and Terra MODIS Satellite Imageries Using Google Earth Engine. *International Journal of Geoinformatics*, Vol. 18(5), 1–12. https://doi.org/10.52939/ijg.v18i5.2365.

[9] Moazzam, M. and Lee, B. (2023). Elevation-Wise and Direction-Wise Distribution of Land Surface Temperature in Jeju Island using Landsat 7 Data. *International Journal of Geoinformatics*, Vol. 19(9), 13–20. https://doi.org/10.52939/ijg.v19i9.2825.

[10] Mostafa, K. M., (2023). Evaluating the Spatiotemporal Dynamics of Land Surface Temperature in Relation to the Land Use/Land Cover changes in Nag-Hammadi District, Egypt, using Remote Sensing and GIS. *International Journal of Geoinformatics*, Vol. 19(3), 13–29. https://doi.org/10.52939/ijg.v19i3.2599.

[11] Faisal, A. A., Kafy, A. A., Rakib, A. A., Akter, K. S., Dewan, M. A. J., Sikdar, M. S., Ashrafi, T. J., Mallik, S. and Rahman, M. M., (2020). Study for Predicting Land Surface Temperature (LST) Using Landsat Data: A Comparison of Four Algorithms. *Advances in Civil Engineering*. https://doi.org/10.1155/2020/7363546.

[12] Mnustafa, E. K., Liu, G., Cao, Y. G., Kaloop, M., Beshr, A. A. A. and Zarzoura, F., (2020). Assessing and Predicting Land Use/Land Cover, Land Surface Temperature and Urban Thermal Field Variance Index Using Landsat imagery for Dhaka Metropolitan Area. *Environmental Challenges.* Vol. 4, https://doi.org/10.1016/j.envc.2021.100192.

[13] Aldileemi, H., Zhran, M. and El-Mewafi, M., (2023). Geospatial Monitoring and Prediction of Land Use/Land Cover (LULC) Dynamics Based on the CA-Markov Simulation Model in Ajdabiya, Libya. *International Journal of Geoinformatics*. Vol. 19(12), 15-29. https://doi.org/10.52939/ijg.v19i12.2973.

[14] Peng, X., Wu., W., Zheng, Y., Sun, J., Hu, T. and Wang, P., (2020). Correlation Analysis of Land Surface Temperature and Topographic Elements in Hangzhou, China. *Sci Rep*., Vol. 10(1)1, https://doi.org/10.1038/s41598-020-67423-6.

[15] Benchelha, M., Benzha, F. and Rhinane, H., (2021). Modeling Urban Growth and Land-Use changes using GIS Based Cellular Automata: Case of Benslimane in Morocco. *International Journal of Geoinformatics*. Vol. 17(6), 1-14. https://journals.sfu.ca/ijg/index.php/journal/article/view/2057.

[16] Chopra, R. and Singh, T., (2022). Urban Heat Island Studies and its Effects Across the Different Cities of the India – A Review. *International Journal of Geoinformatics*. Vol.18(2), 17-27. https://journals.sfu.ca/ijg/index.php/journal/article/view/2147.

[17] García, D. H., Riza, M. and Díaz, J. A., (2023). Land Surface Temperature Relationship with the Land Use/Land Cover Indices Leading to Thermal Field Variation in the Turkish Republic of Northern Cyprus. *Earth Systems and Environment*. Vol. 7(2), 561–580. https://doi.org/10.1007/s41748-023-00341-5.

[18] Sameh, S., Zarzoura, F. and El-Mewafi, M., (2022). Automated Mapping of Urban Heat Island to Predict Land Surface Temperature and Land use/cover Change Using Machine Learning Algorithms: Mansoura City. *International Journal of Geoinformatics*. Vol. 18(6), 47-67. https://doi.org/10.52939/ijg.v18i6.2461.

[19] Abdivaitov, K., Strobl, J. and Tynybekova, A., (2023). Agricultural Land Use Dynamics - A Case Study of Kumkurgan District, Uzbekistan. *International Journal of Geoinformatics*. Vol. 19(11), 38-44. https://doi.org/10.52939/ijg.v19i11.2921.

[20] Selanon, P., Puggioni, F., Dejnirattisai, S. and Rutchamart, A., (2022). Towards Inclusive and Accessible Parks in Pathum Thani Province, Thailand. *City Territory and Architecture*. Vol. 9, 1–16. https://doi.org/10.1186/s40410-022-00169-y.

[21] United States Geological Survey. (2023). What are the Band Designations for the Landsat Satellites?. Available: https://www.usgs.gov/faqs/what-are-band-designations-landsat-satellites. [Accessed Jan. 22, 2023].

[22] Sekertekin, A. and Bonafoni, S., (2020). Land Surface Temperature Retrieval from Landsat 5, 7, and 8 Over Rural Areas: Assessment of Different Retrieval Algorithms and Emissivity Models and Toolbox Implementation. *Remote Sens (Basel)*. Vol. 12(2). https://doi.org/10.3390/rs12020294.

[23] Norovsuren, B., Tseveen, B., Batomunkuev, V., Renchin, T., Natsagdorj, E., Yangiv, A. and Mart, Z., (2019). Land Cover Classification Using Maximum Likelihood Method (2000 and 2019) at Khandgait Valley in Mongolia. *IOP Conf Ser Earth Environ Sci*. Vol. 381, https://doi.org/10.1088/1755-1315/381/1/0120 54.

[24] Dibs, H. and Alnajjar, H., (2013). Maximum Likelihood for Land-Use/Land-Cover Mapping and Change Detection Using Landsat Satellite Images: A Case Study 'South of Johor. *International Journal of Computational Engineering Research*. Vol. 3, 26–33. https://www.ijceronline.com/papers/Vol3_issue6/part%202/E0362026033.pdf.

[25] Srivastava, P. K., Han, D., Rico-Ramirez, M. A., Bray, M. and Islam, T., (2012). Selection of Classification Techniques for Land Use/Land Cover Change Investigation. *Advances in Space Research*. Vol. 50(9), 1250-1265. https://doi.org/10.1016/j.asr.2012.06.032.

[26] Agus, F., Prafanto, A. and Kamil, Z. A., (2023). Detecting Land Use Land Cover Using Supervised Maximum Likelihood Algorithm on Spatiotemporal Imagery in Samarinda, Indonesia. *3rd International Seminar of Natural Resources and Environmental Management 2023*, IOP. https://doi.org/10.1088/1755-1315/1266/1/012085

[27] Ghaleb, F., Mario, M. and Sandra, A. N., (2015). Regional Landsat-Based Drought Monitoring from 1982 to 2014. *Climate*., Vol. 3(3), 563-577. https://doi.org/10.3390/cli3030563.

[28] Balew, A., and Korme, T. (2020). Monitoring land surface temperature in Bahir Dar city and its surrounding using Landsat images. *The Egyptian Journal of Remote Sensing and Space Science*. Vol. 23(3), 371-386. https://doi.org/10.1016/j.ejrs.2020.02.001.

[29] Neinavaz, E., Skidmore, A. K. and Darvishzadeh, R., (2020). Effects of Prediction Accuracy of the Proportion of Vegetation Cover on Land Surface Emissivity and Temperature using the NDVI Threshold Method. *International Journal of Applied Earth Observation and Geoinformation*. Vol. 85, https://doi.org/10.1016/j.jag.2019.101984.

[30] Kaiser, E. A., Rolim, S. B. A., Grondona, A. E. B., Hackmann, C. L., de Marsillac Linn, R., Käfer, P. S., da Rocha, N. S. and Diaz, L. R., (2022). Spatiotemporal Influences of LULC Changes on Land Surface Temperature in Rapid Urbanization Area by Using Landsat-TM and TIRS Images. *Atmosphere (Basel)*. Vol. 13(3). https://doi.org/10.3390/atmos13030460.

[31] Sobrino, J. A., Jiménez-Muñoz, J. C. and Paolini, L., (2004). Land Surface Temperature Retrieval from LANDSAT TM 5. *Remote Sens Environ*., Vol. 90(4), 434–440. https://doi.org/10.1016/j.rse.2004.02.003.

[32] Portela, C. I., Massi, K. G., Rodrigues, T. and Alcântara, E., (2020). Impact of Urban and Industrial Features on Land Surface Temperature: Evidences from Satellite Thermal Indices. *Sustain Cities Soc*. Vol. 56. https://doi.org/10.1016/j.scs.2020.102100.

[33] Guha, S., Govil, H., Dey, A. and Gill, N., (2018). Analytical Study of Land Surface Temperature with NDVI and NDBI using Landsat 8 OLI and TIRS Data in Florence and Naples City, Italy. *Eur J Remote Sens*., Vol. 51(1), 667–678. https://doi.org/10.1080/22797254.2018.1474494.

[34] Null, J., (2023). El Niño and La Niña Years and Intensities. Available: https://ggweather.com /enso/oni.htm. [Accessed Jan. 22, 2023].

[35] Kirtphaiboon, S., Wongwises, P., Limsakul, A., Sooktawee, S. and Humphries, U., (2014). Rainfall Variability over Thailand Related to the El Nino-Southern Oscillation (ENSO). *Journal of Sustainable Energy & Environment*. Vol. 5, 34–42. https://www.jseejournal.com/media/163/attachment/Rainfall%20Variability%20over%20Thailand%20pp.%2037-42.pdf.

[36] Trakolkul, C., Charoenphon, C. and Satirapod, C., (2022). Impact of El Niño–Southern Oscillation (ENSO) on the Precipitable Water Vapor in Thailand from Long Term GPS Observation. *International Journal of Geoinformatics*. Vol. 18(3), 13–20. https://doi.org/10.52939/ijg.v18i3.2197.

[37] Chen, S. and Peake, W., (1961). Apparent Temperatures of Smooth and Rough Terrain. *IRE Transactions on Antennas and Propagation*. Vol. 9(6), 567–572. https://doi.org/10.1109/TAP.1961.1145062.

[38] Beek, M. V., (2015). How does Color Affect Heat Absorption?. Available at: https://www.discoveryexpresskids.com/blog/how-does-color-affect-heat-absorption. [Accessed Jan. 22, 2023].

[39] Science Buddies Staff, (2023), How Does Color Affect Heating by Absorption of Light?. Available at: https://www.sciencebuddies.org/science-fair-projects/project-ideas/Phys_p030/physics/how-does-color-affect-heating-by-absorption-of-light. [Accessed Jan. 22, 2023].